Photochemistry of carboxylic acids containing the phenyl and thioether groups: Steady-state and laser flash photolysis studies

Piotr Filipiak [a], Gordon L. Hug [b], Bronislaw Marciniak [a],*

[a] *Faculty of Chemistry, Adam Mickiewicz University, 60-780 Poznan, Poland*
[b] *Radiation Laboratory, University of Notre Dame, Notre Dame, IN 46556, USA*

Abstract

The mechanisms for the direct photolysis of phenylthioacetic acid (PTAA) and *S*-benzylthioglycolic acid (SBTGA) in acetonitrile were investigated using steady-state and laser flash photolysis. For both compounds, a variety of stable photoproducts were found under steady-state, 254 nm irradiation of acetonitrile solutions. The products from the direct photolysis of PTAA included carbon dioxide (photodecarboxylation), acetic acid, diphenyl disulfide, diphenyl sulfide, thiophenol, thioanisole, di(phenylthio) methane, and *S*-phenyl benzenethiosulfate. The products from the direct photolysis of SBTGA included carbon dioxide, toluene, dibenzyl, dibenzyl sulfide, dibenzyl disulfide, thioglycolic acid, benzyl mercaptan, benzyl alcohol, and benzaldehyde. These stable photoproducts were identified and characterized using HPLC, GC, GC–MS, and UV–vis methods. Quantum yields were determined for the formation of the various stable products following steady-state irradiations in the absence and in the presence of oxygen. In laser flash photolysis (266 nm Nd:YAG laser) experiments, a variety of transients (e.g., phenylthiyl radical, benzyl radical, etc.) was found. For both substrates (PTAA and SBTGA), photoinduced C−S bond cleavage was the main primary process. It was also found that for both acids, photoinduced C−C bond cleavage occurred, but as a minor process relative to C−S bond cleavage. Detailed mechanisms of the primary and secondary processes are proposed and discussed. The validity of these proposed mechanisms was supported by an analysis of the quantum yields of stable products and their transient precursors. Supplementary observations on reactions between the radicals (e.g., $C_6H_5-S^\bullet$, $C_6H_5-{}^\bullet CH_2$) and oxygen are also consistent with the proposed mechanisms.
© 2005 Elsevier B.V. All rights reserved.

Keywords: Phenylthioacetic acid; *S*-Benzylthioglycolic acid; Photolysis; Bond cleavage; Radicals; Quantum yield

1. Introduction

Carbon–sulfur bonds are relatively weak in general [1,2], and these bonds are known to be susceptible to photoinduced cleavage [3–5]. The reactivity at these bonds has proven to be a double-edged sword. On one side, it is of concern to pharmaceutical chemists that are synthesizing sulfur-containing peptides and proteins, where oxidative stability of these drugs can be disappointingly poor [6,7]. On the other side, novel synthetic pathways are accessible through the photochemistry of organic sulfur compounds, and these methodologies have been exploited in past years [8,9]. Of particular interest are the possibilities for photochemistry leading to heterolytic cleavage with subsequent ionic pathways to new syntheses [3].

Recently, triplet sensitization of aromatic carboxylic acids containing thioether groups was used to generate competitively a variety of S-centered radicals and C-centered radicals via competitive bond cleavages [10–12]. The specific application in those works was to understand why organic thioethers were so efficient in functioning as co-initiators in photopolymerization [10,13,14]. However, a subsidiary issue arose as to the branching ratio of C−C versus C−S bond cleavage because C-centered radicals were more efficient initiators of the polymerizations in question [10]. Assessing competitive C−S and C−C bond cleavage in the above studies was masked by electron transfer to the triplet sensitizer from the sulfur compound [15].

A more direct way to investigate the competitive channeling of excess energy to labile bonds in multifunctional compounds is through direct photochemistry. An initial study along these lines has been published on direct photolysis mechanisms of the sulfur-containing carboxylic acid, 4-(methylthio)phenylacetic acid (4-MTPA) [16]. In the present work, the mechanisms of direct photolysis of the sulfur-containing carboxylic acid, phenylthioacetic acid (PTAA) and S-benzylthioglycolic acid (SBTGA) are elucidated.

2. Experimental

2.1. Materials

Phenylthioacetic acid, $C_6H_5–S–CH_2–COOH$, and S-benzylthioglycolic acid, $C_6H_5–CH_2–S–CH_2–COOH$ were purchased both from Aldrich and Lancaster. 4-Carboxybenzophenone (CB) was from Aldrich. Diphenyl disulfide, thiophenol, thioanisole, di(phenylthio) methane, toluene, dibenzyl, dibenzyl sulfide, dibenzyl disulfide, thioglycolic acid ($HS–CH_2–COOH$), and benzaldehyde were purchased from Aldrich. The deionized water for laser flash photolysis was purified in a reverse osmosis/deionization water system from Serv-A-Pure Co. The deionized water for the steady-state analysis came from a water-purification system provided by a Millipore (Simplicity^{TM}) Co. Acetonitrile (for spectroscopy) was purchased both from Merck and J.T. Baker.

2.2. Steady-state photolysis: analysis of stable products and determination of quantum yields

Steady-state photolysis experiments were carried out in $1 cm \times 1 cm$ rectangular UV cells on a standard optical-bench system. A low-pressure mercury lamp (Original Hanau TNN 15 W) was used as the excitation source for 254 nm irradiation. Solutions of PTAA (8.4 mg) and of SBTGA (9.55 mg) in acetonitrile (25 ml) were purged with high-purity argon (30 min) or oxygen (15 min) and then irradiated. Irradiated solutions were analyzed when the conversions of substrates were approximately 30% complete, i.e., 10–20 min of irradiation as monitored by high-pressure liquid chromatography (HPLC) analysis.

UV–vis spectra were measured at room temperature using both a diode array spectrophotometer HP 8452A and a Cary 300 Bio Varian spectrophotometer.

The photolysis of PTAA and SBTGA were monitored by HPLC using a Waters 600E Multisolvent Delivery System pump described previously [16]. The detection system consisted of a Waters 996 photodiode array UV–vis detector. Analytical HPLC was carried out on a Waters XTerra RP$_{18}$ reverse phase column (4.6 mm × 250 mm, 5 μm particle size). Two different eluents were employed. The first eluent system was as follows: the initial phase was a phosphate buffer (60%) and acetonitrile (40%). It was used for the first 4 min. This medium was followed by a gradient, in which the eluent medium changed continuously over a 20 min period until it was 40% phosphate buffer phase and 60% acetonitrile. Finally, the eluent was changed back to the initial phase in the course of 6 s. The flow rate was 1 ml min^{-1}, with optical detection at 240 nm for PTAA. The second eluent system consisted of a phosphate buffer (37%) and acetonitrile (63%) with a flow rate of 1 ml min^{-1} and optical detection at 211 and 250 nm for SBTGA. HPLC–MS analyses were performed on this same system using a ZQ (electrospray) mass detector (Waters and Micromass).

Gas chromatographic (GC) analyses were performed on a Hewlett-Packard 5890 II series instrument equipped both with FID and TCD detectors in order to quantify CO_2 and also to identify stable products formed during steady-state photolysis. Analyses were done with both HP–HFAP and ULTRA 1 capillary columns (0.32 mm × 25 m) using a temperature program operating between 120 and 220 °C (heating rate, 10 °C min^{-1}) and a flow rate of 1.5 ml min^{-1}. GC–MS analyses were performed on a Varian Saturn 2100 T instrument equipped with an ion trap. Analyses were done with a DB-5 capillary column (30 m).

The quantum yields, Φ, were measured using uranyl oxylate actinometry at 254 nm taking its quantum yield to be 0.602 [17].

2.3. Laser flash photolysis

The nanosecond laser flash photolysis and its data acquisition system have been previously described in detail [18,19]. The Nd:YAG laser (PRO 230, Quanta-Ray Co.) provides 10–12 ns pulses. For the experiments described herein, the laser was operated at 266 nm and 10–12 mJ/pulse. The transients were monitored with a pulsed 1 kW xenon lamp, having the monitoring beam perpendicular to the laser beam. All experiments were carried out with a gravity-driven flow system and a rectangular quartz optical cell (0.5 cm × 1 cm). The monitoring-light pathlength was 0.5 cm. A solution of CB (2 mM) at neutral pH was used as a relative actinometer [20] by monitoring its triplet–triplet absorption ($\varepsilon_{535} = 6250 M^{-1} cm^{-1}$) [21].

3. Results and discussion

3.1. Steady-state photolysis

The UV–vis absorption spectrum presented in Fig. 1a (PTAA) is very similar to the spectrum of thioanisole [22]. Based on this similarity to thioanisole ($\lambda_{max} = 254 nm$), the absorption band of PTAA ($\lambda_{max} = 250 nm$), in the neighborhood 250 nm, can be attributed to a π–π* transition [23]. On the other hand, the UV–vis absorption spectrum presented in Fig. 1b (SBTGA) is similar to the spectrum of benzyl methyl sulfide [24].
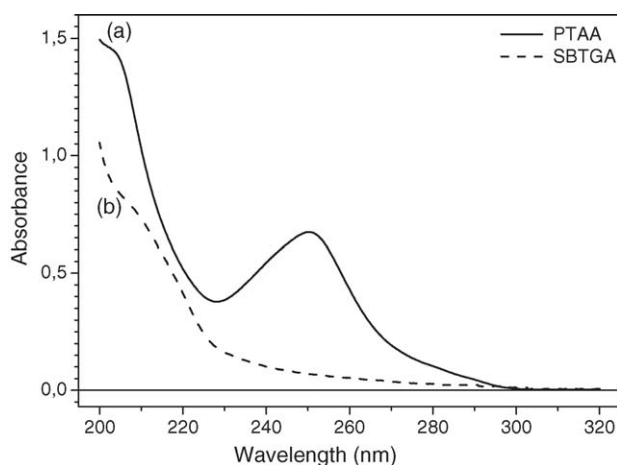
Fig. 1. UV–vis absorption spectra of: (a) 0.1 mM PTAA and (b) 80 μM SBTGA in acetonitrile taken in 1 cm UV cell.

3.1.1. Direct photolysis of phenylthioacetic acid

Solutions of PTAA in acetonitrile were irradiated in the absence and presence of oxygen. The spectrophotometric changes were monitored by taking UV–vis spectra at regular time intervals. The resulting spectra show only small changes in the absorption band between 230 and 260 nm. This indicates that any products formed during the photolysis absorbed in the same spectral region, where PTAA absorbs. Consistent with this, the post-irradiation spectra showed the small development of an absorption band between 280 and 320 nm.

GC–MS chromatography and HPLC were used for the identification of stable products formed during the direct steady-state photolysis of PTAA. Oxygen-free acetonitrile solutions of 24 mM PTAA were irradiated at 254 nm for 150 min and analyzed by GC–MS. A typical GC–MS chromatogram (Fig. 2a) shows a variety of primary and secondary
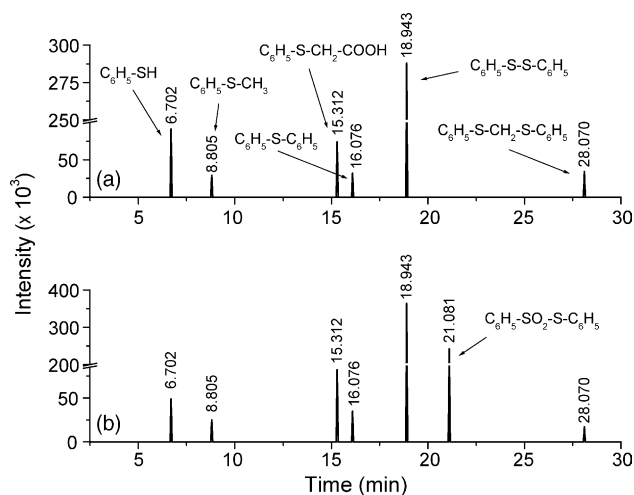

Fig. 2. (a) GC–MS chromatogram recorded after a 150 min irradiation of PTAA (24 mM) in Ar-saturated acetonitrile. (b) GC–MS chromatogram recorded after a 120 min of irradiation of PTAA (24 mM) in O$_2$-saturated acetonitrile.
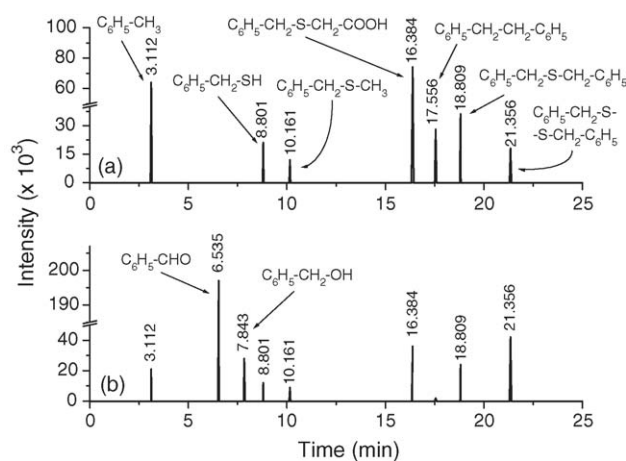

Fig. 3. (a) GC–MS chromatogram recorded after a 75 min irradiation of SBTGA (10 mM) in Ar-saturated acetonitrile. (b) GC–MS chromatogram recorded after an 80 min of irradiation of SBTGA (10 mM) in O$_2$-saturated acetonitrile.
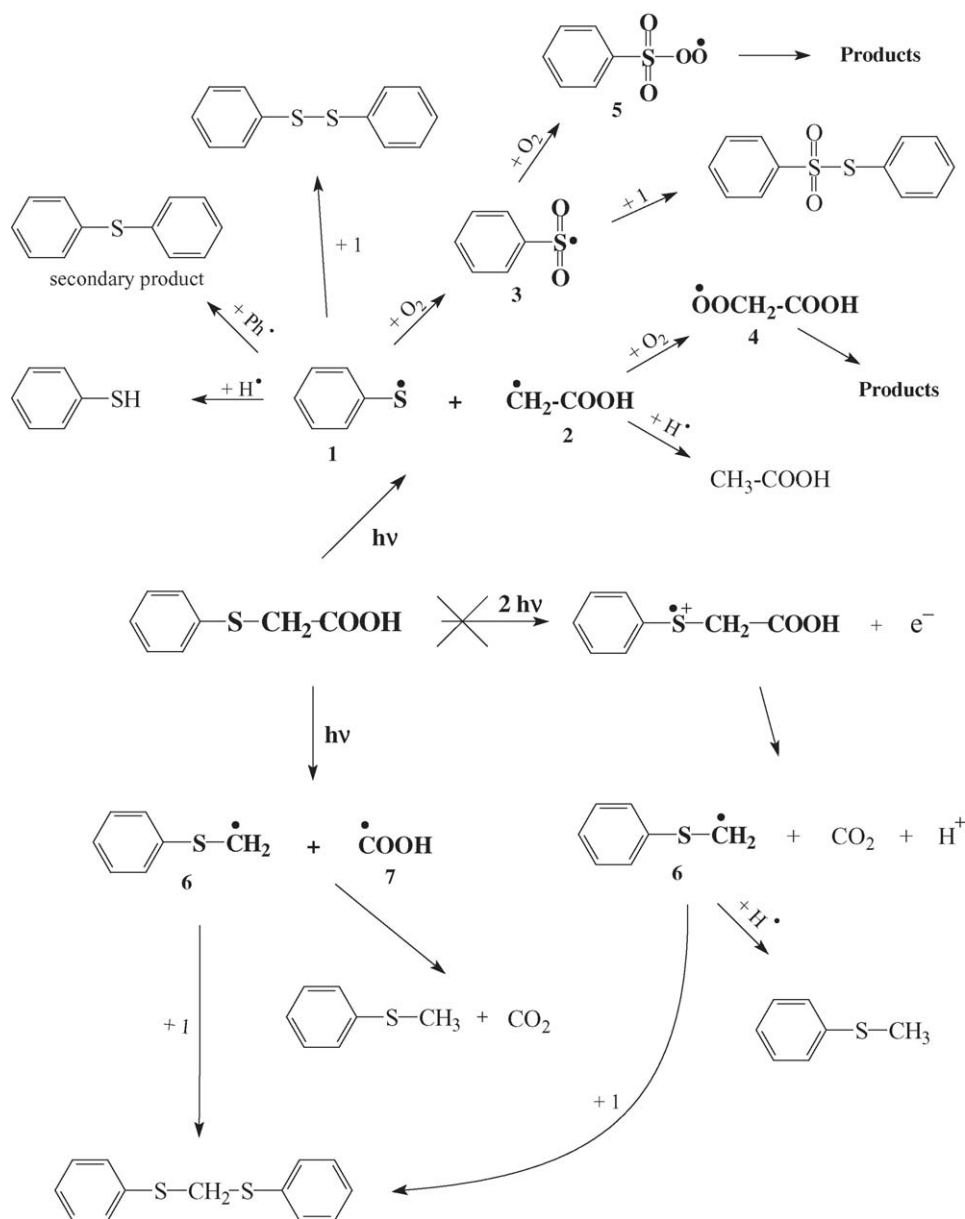
stable photoproducts; these same products were detected in the HPLC analysis of the same irradiated solutions.

A similar analysis was performed, following irradiation, of oxygen-saturated acetonitrile solutions of PTAA. The resulting chromatogram showed a new photoproduct (Fig. 2b) that appeared in quite large concentrations following 120 min of irradiation. This additional stable photoproduct that was observed in irradiated oxygen-saturated acetonitrile solution, was identified as *S*-phenyl benzenethiosulfate, C_6H_5–SO_2–S–C_6H_5. Supplementary gas chromatographic (GC) analyses were performed in order to identify acetic acid and CO_2, and to quantify the quantum yield of carbon dioxide formation. Scheme 1 shows all the stable photoproducts (primary and secondary) formed during the direct photolysis of PTAA. One of the products (diphenyl sulfide) was detected in trace amounts after prolonged irradiation, which indicates that it results from secondary reaction(s) under our irradiation conditions.

3.1.2. Direct photolysis of S-benzylthioglycolic acid

Solutions of SBTGA in acetonitrile were irradiated in the absence and presence of oxygen. As in the case of PTAA, the spectrophotometric changes of the irradiated solutions were monitored by taking UV–vis spectra at regular time intervals. The resulting spectra show the small development of an absorption band between 240 and 270 nm and almost no changes around 210 nm, which indicates that any products absorb in the same region as does SBTGA itself.

GC–MS chromatography and HPLC were used for the identification of stable products formed during the direct steady-state photolysis of SBTGA. Oxygen-free acetonitrile solutions of 10 mM SBTGA were irradiated at 254 nm for 75 min and were analyzed by GC–MS. A typical GC–MS chromatogram (Fig. 3a) shows a variety of stable photoproducts. These same products were detected in the HPLC analysis of the irradiated solutions.
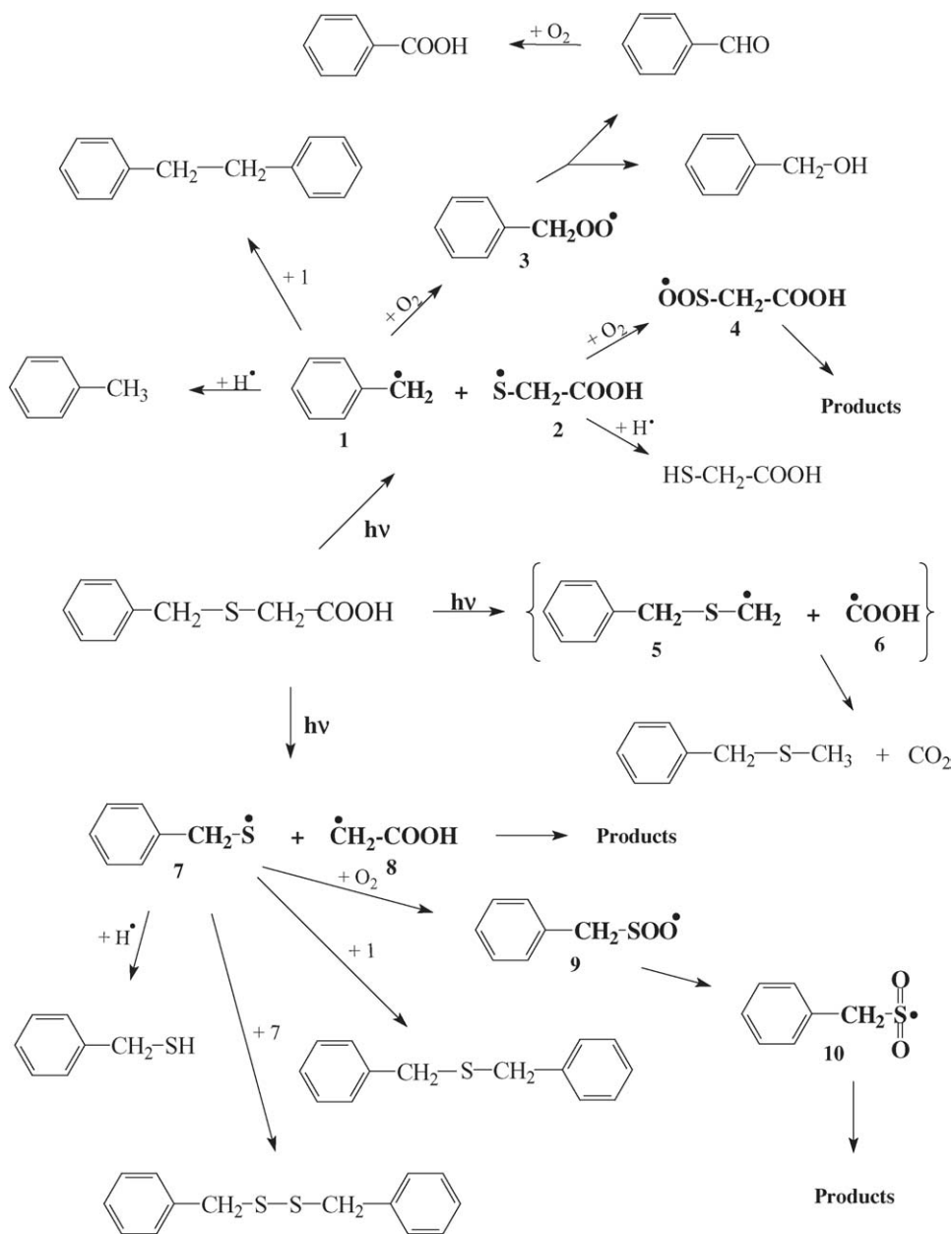
Scheme 1.

A similar analysis was performed following irradiation of oxygen-saturated acetonitrile solutions of SBTGA. The resulting chromatograms showed different photoproducts (Fig. 3b). These products, from oxygen-saturated solutions, appear in quite large concentrations following 80 min of irradiation. The additional stable photoproducts that were identified in irradiated oxygen-saturated acetonitrile were benzaldehyde, C_6H_5–CHO, and benzyl alcohol, C_6H_5–CH_2–OH. Supplementary gas chromatographic (GC) analyses were performed in order to identify CO_2 and to quantify its yield. Using the HPLC system, an additional product was found. It was identified as thioglycolic acid, HS–CH_2–COOH. All of the stable photoproducts formed during the direct photolysis of SBTGA are shown in Scheme 2.

3.1.3. Quantum yield determinations

Since standard samples of the major products (vide supra), were commercially available, it was possible to determine the photoproducts' quantum yields by calibrating the various chromatographic methods. For the photochemical quantum yield determinations, the initial concentrations of PTAA were varied from 1.6 to 2.2 mM, and the initial concentrations of SBTGA were varied from 1.5 to 2.8 mM, all in acetonitrile. The changes, Δc, in the concentrations of substrate and the various stable photoproducts were determined both by GC and HPLC measurements using the authentic compounds as concentration standards. All quantum yields were extrapolated back to zero percent conversion of substrate in order to get the initial quantum yields. These procedures were necessary because of the absorption of the photolytic light by the

Scheme 2.

photoproducts. Quantum yields determined by these methods are presented in Table 1 (PTAA) and in Table 2 (SBTGA). It can be seen from Tables 1 and 2 that in the presence of oxygen, most of the quantum yields (decomposition of PTAA and formation of products from both PTAA and SBTGA) change significantly as compared to the deaerated systems. The participation of oxygen in the reaction mechanism is discussed below.

Table 1
Quantum yields for the decomposition of phenylthioacetic acid (PTAA) and formation of primary photoproducts[a] in steady-state photolysis at 254 nm in acetonitrile[b]

	PTAA	C_6H_5–SH	C_6H_5–S–S–C_6H_5	C_6H_5–S–CH_3	CO_2	C_6H_5–S–CH_2–S–C_6H_5
+Ar	0.19	0.054	0.047	0.001	0.02	0.002
+O_2	0.29	0.002	0.029	–	×	≤0.002

(×) Not determined.
[a] From steady-state measurements, extrapolated to zero percent conversion of PTAA, estimated errors ± 10%.
[b] [PTAA] = 1.62–2.16 mM; I_0 = (1.9–2.9) × 10^{-4} einstein × dm^{-3} × min^{-1}.

Table 2
Quantum yields for the decomposition of *S*-benzylthioglycolic acid (SBTGA) and formation of primary photoproducts[a] in steady-state photolysis at 254 nm in acetonitrile[b]

	SBTGA	C_6H_5–CH_3	C_6H_5–CHO	C_6H_5–CH_2–CH_2–C_6H_5	C_6H_5–CH_2–S– CH_2–C_6H_5	C_6H_5–CH_2–S–S– CH_2–C_6H_5	HS–CH_2–COOH	CO_2
+Ar	0.30	0.025	<0.01	0.011	0.028	0.005	0.19	0.03
+O_2	0.29	0.046	0.16	–	0.01	0.003	×	×

(×) Not determined.

  [a] From steady-state measurements, extrapolated to zero percent conversion of SBTGA, estimated errors $\pm$ 10%.

  [b] [SBTGA] = 1.49–2.8 mM; $I_0 = (1.9$–$2.65) \times 10^{-4}$ einstein $\times$ dm^{-3} $\times$ min^{-1}.

3.2. Reference spectra

From the presence of formal C–C bond cleavage products (C_6H_5–S–CH_3 and C_6H_5–S–CH_2–S–C_6H_5), we anticipated that the C-centered radical, C_6H_5–S–$^\bullet CH_2$, would be formed following the nanosecond laser flash photolysis of PTAA. The reference spectrum for this radical was obtained previously [25,26] in the pulse radiolysis of PTAA, where this radical was formed following the decarboxylation of the sulfur-centered radical zwitterion, C_6H_5–$S^{\bullet+}$–CH_2–COO^-. The reference spectrum of the C-centered radical, C_6H_5–S–$^\bullet CH_2$, is characterized by an absorption band with a maximum at $\lambda_{max} = 330$ nm, $\varepsilon_{330} = 3800$ M^{-1} cm^{-1} [26]. We could not obtain the reference spectrum for the sulfur-centered radical zwitterions because of their short lifetime (about 1 μs) [15]. From the presence of formal C–S bond cleavage products (e.g., C_6H_5–SH and C_6H_5–S–S–C_6H_5), we anticipated that the S-centered radical, C_6H_5–$^\bullet S$, would be formed following the nanosecond laser flash photolysis of PTAA. We assigned the transient absorption observed at 490 nm (see Fig. 4) as the C_6H_5–$^\bullet S$ radical based on the literature spectra determined by Ioele et al. [26] ($\varepsilon_{460} = 1800$ M^{-1} cm^{-1} in water) and Ouchi et al. [27] ($\varepsilon_{490} = 2000$ M^{-1} cm^{-1}

Fig. 4. Transient absorption spectra following 266 nm laser flash photolysis of C_6H_5–S–CH_2–COOH (PTAA) (0.2 mM) in Ar-saturated acetonitrile recorded at four different delays times, relative actinometry: [T] = 25.4 μM. Inset shows experimental trace for decays taken at: (a) 300 nm and (b) 460 nm.

in tetrahydrofuran). For our calculations, we used $\varepsilon_{490} = 2000$ M^{-1} cm^{-1}.

The presence of *S*-phenyl benzenethiosulfate, C_6H_5–SO_2–S–C_6H_5 among the steady-state photoproducts indicates that in oxygen-saturated solution, the C_6H_5–$^\bullet S$–OO radical was formed, but the spectrum of this specific radical has not been determined. For identification and estimation of this radical's quantum yield of formation, we took the reference spectra for a similar radical, *p*-H_3C–C_6H_4–$^\bullet S$–OO, which was measured by Chatgilialoglu et al. [28] and by Eriksen and Lind [29] ($\varepsilon_{335} = 1200$ M^{-1} cm^{-1} in CCl_4).

In the photolysis of SBTGA, we were expecting to produce the sulfur-centered radical cation, C_6H_5–CH_2–$S^{\bullet+}$–CH_2–COOH, and the C-centered radicals, C_6H_5–$^\bullet CH_2$, and C_6H_5–CH_2–S–$^\bullet CH_2$. The latter radical was observed following the decarboxylation of C_6H_5–CH_2–$S^{\bullet+}$–CH_2–COO^- [15]. As in the case of PTAA, we were not able to detect any absorption from the sulfur-centered radical cation of SBTGA, presumably, because its lifetime is too short [15]. The radical zwitterion decays into at least two different C-centered radicals (C_6H_5–$^\bullet CH_2$, and C_6H_5–CH_2–S–$^\bullet CH_2$) that are likely present in the same time and spectral ranges. Thus, it was not valid to use the observed spectrum as a reference spectrum, because it was composed from at least these two intermediates. For further computations, on this system, we used the benzyl radical spectrum from Hugemann and Schwarz [30] ($\varepsilon_{317} = 12,000$ M^{-1} cm^{-1} in cyclohexane). For the reference spectrum of the benzylthiyl radical, C_6H_5–CH_2–$S^\bullet$, we used the spectrum determined by Wendenburg et al. [31] ($\varepsilon_{410} = 10,000$ M^{-1} cm^{-1} in tetrahydrofuran at 77 K).

3.3. Nanosecond laser flash photolysis

3.3.1. Flash photolysis of phenylthioacetic acid

Solutions of 0.2 mM PTAA in acetonitrile were irradiated with 10 ns pulses from the fourth harmonic (266 nm) of a Nd:YAG laser. Transient absorption was seen in the region of 280–700 nm in argon-saturated solutions (see Fig. 4). The transient spectra shown in Fig. 4 were assembled from kinetic traces and displayed at a few selected time delays (between 60 ns and 60 μs) following the laser pulse. Inset (a) in Fig. 4 shows a 300 nm kinetic trace on an 80 μs time scale. This kinetic trace cannot be fit to a single exponential decay. From the steady-state products and the reference spectra of the products' likely precursor radicals, we suspect
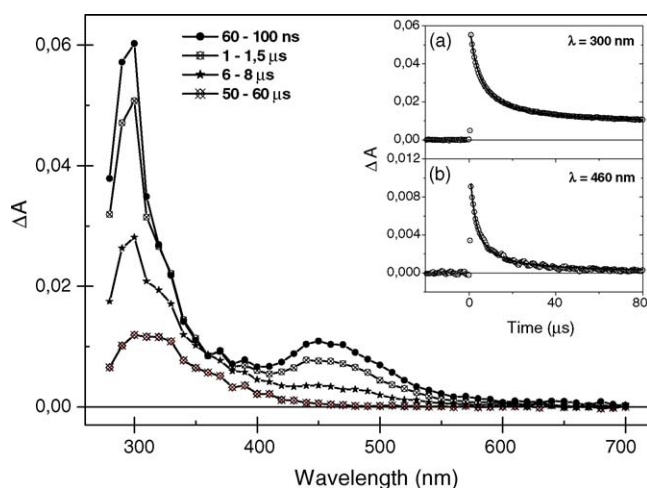
that there are at least three different transients absorbing at 300 nm. The three species are $C_6H_5-{}^\bullet S$, $C_6H_5-S-{}^\bullet CH_2$, and ${}^\bullet CH_2-COOH$. Thus, it would have been difficult to get reliable quantitative results on the individual species from this spectral region.

On the same time scale, the kinetic trace at 460 nm (inset, Fig. 4b) shows a second-order decay with a half-life of $\tau_{1/2} = 2.1\,\mu s$. Of the possible radicals, it is the $C_6H_5-{}^\bullet S$ radical that is assigned as being responsible for the absorption at 460 nm [26]. From the kinetic trace at 460 nm, it was possible to estimate the recombination rate constant for phenylthiyl radicals. For this estimation, Eq. (1) was used [32].

$$2k = a\varepsilon l \tag{1}$$

where $2k$ is the radicals' recombination rate constant $[M^{-1}\,s^{-1}]$, $a = 2k/\varepsilon l$ a fitting parameter from a non-linear least-squares fit to a second-order decay function, ε the extinction coefficient ($\varepsilon_{490} = 2000\,M^{-1}\,cm^{-1}$ in tetrahydrofuran [27]) at the observed wavelength, and l is optical pathway equal to 0.5 cm. The recombination rate constant so determined is ($2k = 4.6 \times 10^{10}\,M^{-1}\,s^{-1}$), for acetonitrile solution which can be compared to the literature values [33–35] (($2k = 2–3 \times 10^9\,M^{-1}\,s^{-1}$) for aqueous solutions. The computed value, in excess of the diffusion-controlled value ($1.9 \times 10^{10}\,M^{-1}\,s^{-1}$) in acetonitrile [17], indicates that cross-radical reactions may be operative (see Section 3.4) below for indirect evidence of cross-radical reactions involving ${}^\bullet CH_2-COOH$. If cross-radical reactions were operating, our calculation of the effective c_0 from optical measurements would be too small leading to an over-estimation of $2k$, which is computed from the product $2kc_0$ (see Eqs. (2) and (3) below).

The spectra shown in Fig. 5 (for an oxygen-saturated solution of PTAA) are generated from kinetic traces and displayed
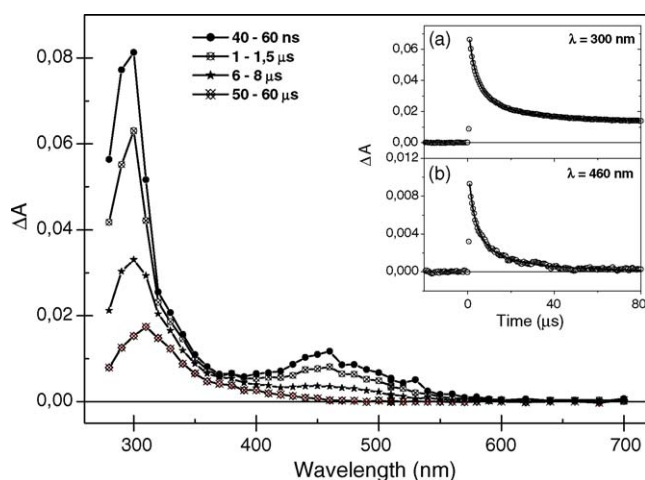
at several selected time delays (between 40 ns and 60 μs) following the laser pulse. Generally the spectra shown in Fig. 5 are very similar to those in Fig. 4. Inset (a) in Fig. 5 shows a 300 nm kinetic trace that represents the decay of all three transients suggested (see above) as being present in argon-saturated solutions and one new transient, the S-centered radical ($C_6H_5-{}^\bullet S-OO$) formed from peroxide radical ($C_6H_5-S-OO^\bullet$). It was not possible to get reliable results on the individual species from this spectral region.

The kinetic trace at 460 nm for phenylthiyl radical (inset, Fig. 5b) shows a decay similar to that observed for Ar-saturated solutions of PTAA in acetonitrile. We still observed fast decay of the 460 nm absorption band when oxygen was present. However, the decay can no longer be fit well with a simple second-order decay function. The decay fits very well to a mixed decay (first and second order). This is consistent with the phenylthiyl radicals ($C_6H_5-{}^\bullet S$) reacting with themselves and other radicals via second-order reactions plus additional pseudo-first-order reactions, e.g., with oxygen although aromatic thiyl radicals normally react slowly with oxygen [36,37] ($k \sim 10^4\,M^{-1}\,s^{-1}$).

We could not accurately resolve the spectra of the various C- and S-centered radicals since their absorption spectra clustered at the edge of our effective spectral window of observation, which was limited by the absorption of the substrate itself. It was only possible to estimate the quantum yields of the transients taking changes in transient absorbances at appropriate wavelengths in the presence or absence of oxygen. All the quantum yields of the primary products were extrapolated back to time zero (end of laser pulse) in order to ascertain the initial quantum yields.

The quantum yields estimated by this method are presented in Table 3. In spite of the limitations described above, it can be seen from Table 3 that the quantum yields for the formation of $C_6H_5-{}^\bullet S$ radicals ($\sim$0.3) are roughly the same in the presence or absence of oxygen. The phenylthiyl radical is the main primary product in both cases. In the presence of oxygen, the phenylthiyl radical reacts with oxygen to form a peroxide radical that is transformed into the fully S-centered radical [33]. The decay of the phenylthiyl radical in the presence of oxygen showed a mixed decay, radical–radical plus pseudo-first-order that is consistent with this mechanism. Furthermore, the large concentration of the stable photoproduct $C_6H_5-SO_2-S-C_6H_5$ (the main product detected in GC analyses in oxygen-saturated solution) is consistent with the reaction between oxygen and $C_6H_5-{}^\bullet S$ radicals making a significant contribution to phenylthiyl's decay.

It can be seen from the values in Table 1 that the presence of oxygen significantly changes the quantum yields for the decomposition of the substrate (PTAA) and formation of products from the steady-state analysis. On the other hand, the presence of oxygen does not change the quantum yields for the formation of the phenylthiyl radical in the laser flash photolysis experiments. As discussed below, these oxygen effects give critical clues to the mechanism of the direct photolysis.

Fig. 5. Transient absorption spectra following 266 nm laser flash photolysis of $C_6H_5-S-CH_2-COOH$ (PTAA) (0.2 mM), in O_2-saturated acetonitrile, recorded at four different delays times, relative actinometry: $[T] = 25.4\,\mu M$. Inset shows experimental trace for decays taken at: (a) 300 nm and (b) 460 nm.

Table 3
Quantum yields for the decomposition[a] of phenylthioacetic acid (PTAA) in steady-state photolysis at 254 nm and formations of transients[b] in laser flash photolysis at 266 nm in acetonitrile

	PTAA	$C_6H_5-S^{\bullet}$ [c]	$C_6H_5-S^{\bullet}-OO$ [d]	$C_6H_5-S-^{\bullet}CH_2$	$^{\bullet}CH_2-COOH$	CO_2
+Ar	0.19	0.31	–	∼0.02	<0.27	0.02
+O_2	0.29	0.30	≤0.31	<0.01	<0.36	×

(×) Not determined.

[a] From steady-state measurements, extrapolated to zero percent conversion of PTAA, estimated errors ± 10%; [PTAA] = 1.62–2.16 mM; $I_0 = (1.9–2.9) \times 10^{-4}$ einstein × dm^{-3} × min^{-1}.

[b] From laser flash photolysis, estimated values with errors ± 20%; {[PTAA] = 0.2 mM}.

[c] From laser flash photolysis, calculated values with errors ± 10%.

[d] Estimated for delay time 55 μs.

3.3.2. Flash photolysis of S-benzylthioglycolic acid

Solutions of 1.1 mM SBTGA in acetonitrile were irradiated as above with 10 ns laser pulses at 266 nm. Transient absorption was detected between 270 and 450 nm in argon-saturated solutions, and representative transient spectra are shown in Fig. 6. The inset to Fig. 6 shows a 315 nm kinetic trace on a 40 μs time scale. This kinetic trace cannot be fit to a single exponential decay. Several likely radicals absorb at this wavelength. Among them are $C_6H_5-CH_2-S-^{\bullet}CH_2$ ($\varepsilon_{300} = 3400 \, M^{-1} \, cm^{-1}$), $^{\bullet}S-CH_2-COOH$ ($\varepsilon_{330} = 300 \, M^{-1} \, cm^{-1}$) [38], $^{\bullet}CH_2-COOH$ ($\varepsilon_{310} = 310 \, M^{-1} \, cm^{-1}$) [39], and $C_6H_5-^{\bullet}CH_2$ ($\varepsilon_{317} = 12,000 \, M^{-1} \, cm^{-1}$ in cyclohexane) [30]. Assuming that the latter is the main transient and that the long-time absorbance is due to a radical–radical combination product, it was possible to estimate the recombination rate constant for these benzyl radicals using Eq. (2).

$$\varepsilon_c cl + \varepsilon_p pl = \frac{1}{2}\varepsilon_p c_0 l + \left(\varepsilon_c c_0 l - \frac{1}{2}\varepsilon_p c_0 l\right)\frac{1}{1+2kc_0t} \quad (2)$$

where "c" and "p" refer to the radical and combination product, respectively. The left-hand side is the total absorbance of the solution. Three fitting parameters were used:

$$a_1 = \frac{1}{2}\varepsilon_p c_0 l; \quad a_2 = \varepsilon_c c_0 l - \frac{1}{2}\varepsilon_p c_0 l; \quad a_3 = 2kc_0 \quad (3)$$
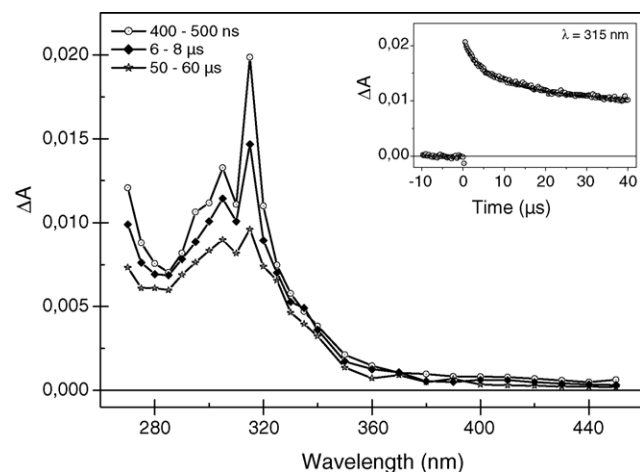
By straightforward algebra, c_0 and ε_p can be eliminated to give:

$$2k = \frac{a_3}{a_1 + a_2}\varepsilon_c l \quad (4)$$

The recombination rate constant so determined would be $2k = 3.8 \times 10^{10} \, M^{-1} \, s^{-1}$ for acetonitrile solutions. Again, this $2k$ is much larger than diffusion-controlled in acetonitrile and considerably different than literature values ($2k = 1.6–3.0 \times 10^9 \, M^{-1} \, s^{-1}$) [40] in aqueous solution and in methanol. We again ascribe this discrepancy to cross-radical reactions.

Transient spectra of oxygen-saturated solutions of SBTGA were generated from kinetic traces in the spectral region 270 – 700 nm (see Fig. 7). Inset (a) in Fig. 7 shows a 315 nm kinetic trace that represents the decay of all the transients identified in argon-saturated solution plus peroxide radicals. However, the benzyl radical is expected to dominate because of its relatively large extinction coefficient in this spectral region. The kinetic trace at 315 nm shows a single exponential decay with a lifetime of $\tau = 33$ ns. It corresponds to the lifetime of the benzyl radical in the presence of oxygen. The estimated rate constant for quenching

Fig. 6. Transient absorption spectra following 266 nm laser flash photolysis of $C_6H_5-CH_2-S-CH_2-COOH$ (SBTGA) (1.1 mM), in Ar-saturated acetonitrile, recorded at three different delays times, relative actinometry: [T] = 14.5 μM. Inset shows experimental trace for decays taken at 315 nm.
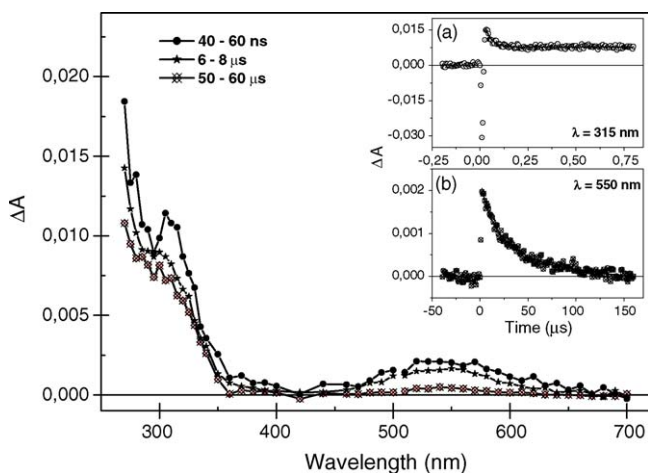

Fig. 7. Transient absorption spectra following 266 nm laser flash photolysis of $C_6H_5-CH_2-S-CH_2-COOH$ (SBTGA) (1.1 mM), in O_2-saturated acetonitrile, recorded at three different delays times, relative actinometry: [T] = 14.5 μM. Inset shows experimental trace for decays taken at: (a) 315 nm, benzyl radical and (b) 550 nm, peroxide radicals.

Table 4
Quantum yields for the decomposition[a] of S-benzylthioglycolic acid (SBTGA) in steady-state photolysis at 254 nm and formations of transients[b] in laser flash photolysis at 266 nm in acetonitrile

	SBTGA	C_6H_5–•CH_2[c]	C_6H_5–CH_2–OO•	C_6H_5–CH_2–S•	•OOS–CH_2–$COOH$	CO_2
+Ar	0.30	0.24	–	~0.02	–	0.03
+O_2	0.29	0.28	≤0.35	~0.01	≤0.32	×

(×) Not determined.

[a] From steady-state measurements, extrapolated to zero percent conversion of SBTGA, estimated errors ± 10%; [SBTGA] = 1.49–2.8 mM; $I_0 = (1.9–2.65) \times 10^{-4}$ einstein × dm^{-3} × min^{-1}.

[b] From laser flash photolysis, estimated values with errors ± 20%; {[SBTGA] = 1.1 mM}.

[c] From laser flash photolysis, calculated values with errors ± 10%.

the benzyl radical by oxygen ($k = 3.3 \times 10^9$ M^{-1} s^{-1}), calculated from the Stern–Volmer equation, is similar to the literature value for this reaction given by Maillard et al. [41] ($k = 3.4 \times 10^9$ M^{-1} s^{-1}). No second-order component was observed under these conditions because of the fast reaction of the C-centered radicals with oxygen.

The kinetic trace at 550 nm (inset, Fig. 7b) shows a first-order decay with a lifetime of about 31 µs. The 550 nm band is assigned to the peroxide radicals (C_6H_5–CH_2–S–OO•, and HOOC–CH_2–S–OO•) [42,43]. They decay into S-centered radicals [33].

Just as in the case of PTAA, we could not accurately resolve the spectra of the various C- and S-centered radicals since their absorption spectra clustered at the edge of our effective spectral window of observation.

The quantum yields estimated by a method similar to that for PTAA are presented in Table 4. It can be seen from Table 4 that the quantum yield for the formation of the C_6H_5–•CH_2 radical is 0.24 in the absence of oxygen, and 0.28 in the presence of oxygen. The complementary radical is the •S–CH_2–$COOH$ radical, which would be formed in a C–S bond cleavage of SBTGA. These two radicals are the main primary species formed in the presence or absence of oxygen. In the presence of oxygen, there are two main secondary radicals formed from the reactions of C_6H_5–•CH_2 and •S–CH_2–$COOH$ radicals with oxygen. Their quantum yields are ~0.35 for the C_6H_5–CH_2–OO• radical and ~0.32 for the •OOS–CH_2–$COOH$ radical (see Table 4). Comparison of these radicals' quantum yields with those of their respective precursors indicates that almost all of the C_6H_5–•CH_2 and •S–CH_2–$COOH$ radicals decay through the reaction with oxygen under the conditions used in these experiments. In both cases (absence or presence of oxygen), the other radicals are present in very small concentrations.
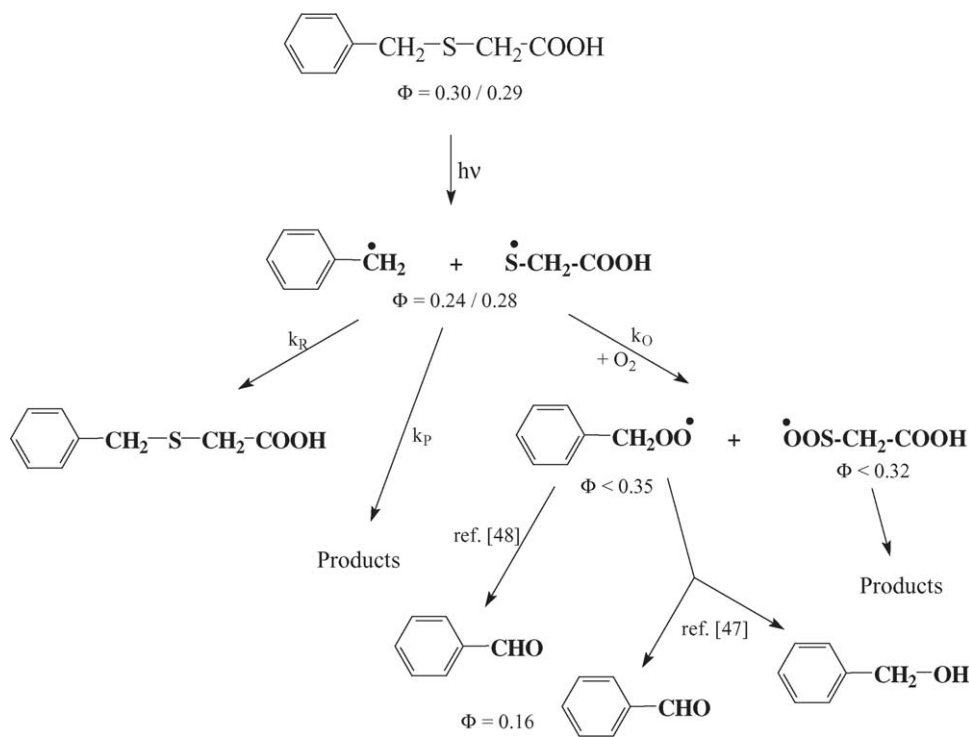
It can be seen from the values in Table 2 that the presence of oxygen significantly changes the quantum yields for the formation of products from steady-state analysis. On the other hand, the presence of oxygen only slightly changes the quantum yields for the formation of the products in laser flash photolysis experiments. This is consistent with the laser flash photolysis reflecting the initial yields of the radicals, which are not dependent on the low concentration of oxygen, whereas the products are the final yields after the radicals react with oxygen. In other words, this indicates that the

radicals are formed in an excited state reaction that is not quenched by oxygen, most likely an excited singlet state. On the other hand, the stable products may be formed on longer time scales where transients have time to be scavenged by the small amount of oxygen present in solution. As discussed below, these oxygen effects give critical clues to the mechanism of the direct photolysis of SBTGA.

3.4. Direct photolysis mechanisms of carboxylic acids containing phenyl and thioether groups

In the direct photolysis of PTAA and SBTGA, a careful examination of the primary photoproducts and their quantum yields (Tables 1 and 2) reveals three general results. First, the photoproducts fall into two groups each of which is derived from a bond cleavage (C–S versus C–C). Second, the presence of oxygen significantly changes all the steady-state quantum yields. Third, the quantum yields indicate that, in the presence and absence of oxygen, C–S bond cleavage is the main primary process. This is consistent with the bond energy, which is larger for C–C bond (338 kJ mol^{-1}) [44], than for C–S bond in thioethers (257–293 kJ mol^{-1}) [32,44,45]. The situation that photoinduced C–S bond cleavage occurred in the presence of oxygen is different from the direct photolysis of 4-(methylthio)phenylacetic acid [16], where we did not observe any C–S bond cleavage in the presence of oxygen (due to efficient quenching of the triplet state of 4-MTPA by oxygen). The lack of oxygen quenching of the quantum yields of transients in PTAA and SBTGA suggests that the bond cleavage is coming from excited singlet states in these two compounds.

A mechanism is proposed in Scheme 1 to rationalize these generalizations for PTAA. Two primary photolytic pathways are possible. The first pathway is a C–S bond cleavage (main reaction) leading to the formation of C_6H_5–•S (Φ ~0.3) and •CH_2–$COOH$ radicals. The second pathway is a C–C bond cleavage leading to formation of C_6H_5–S–•CH_2 (Φ ~0.02) and •$COOH$ radicals. This latter quantum yield corresponds to the quantum yield of carbon dioxide formation (0.02). The C_6H_5–S–•CH_2 and •$COOH$ radicals could be also formed via a mechanism that involves an initial ionization of PTAA leading to formation of the S-centered radical cation (C_6H_5–S•$^+$–CH_2–$COOH$). However, this reaction was not possible in our steady-state experiments because of

Scheme 3.

the high ionization potential of PTAA ($830 \, kJ \, mol^{-1}$) [46], unless it would be a multiphotonic process. Such a multiphotonic process is not likely under our steady-state photolysis conditions because of low probability of two-photonic absorption.

In order to discuss this scheme, we show an abbreviated version of the mechanism for the direct photolysis of PTAA in Scheme 3. This version displays only the main pathway (C–S bond cleavage). After 254 nm irradiation of PTAA, C–S bond cleavage occurs. Following this, there are three possibilities for the fates of the two resulting radicals. First is the recombination reaction (k_r), which leads to the reformation of the substrate. The second possibility involves the reactions between all radicals formed during the photolysis, including dimerization and hydrogen abstraction reactions, leading to formation of the rest of the products (k_p). The third pathway is the reaction with oxygen (k_O).

This third pathway is the critical reaction when oxygen is present. In the absence of oxygen, the quantum yield for the formation of phenylthiyl radicals (~0.31 from Table 3) is significantly larger than the quantum yield for the decomposition of PTAA (0.19 from Table 1). However, when oxygen is present, the substrate's decomposition quantum yield (0.29, Table 1) is the same as the phenylthiyl-radical quantum yield (0.30, Table 3). The rational for this is as follows:

the phenylthiyl radical and the carboxymethyl radical can recombine to reform the substrate or to form other products. When oxygen is absent, the rates constants for all these reactions appear to be almost the same. Thus, the recombination reaction is competitive with the other reactions, and the quantum yield for the decomposition of substrate is only 0.19. However, when oxygen is present, there is one more competitive reaction between the $^{\bullet}CH_2$–COOH radical and oxygen for which the rate constant is quite large ($k = 2$–$5 \times 10^9 \, M^{-1} \, s^{-1}$) [36,41]. Following this reaction with oxygen, the $^{\bullet}CH_2$–COOH radical is effectively removed (trapped) from the system, in the sense that the phenylthiyl radical cannot reform PTAA. Hence, the phenylthiyl radical reacts with the rest of radicals and also with oxygen. This is the reason why the quantum yields for the decomposition of substrate in the presence of oxygen in relatively high (0.29). In both cases (in the presence and absence of oxygen), the quantum yields for the formation of phenylthiyl radical were calculated from the concentration taken at 80 ns after the laser pulse (before non-geminate recombination reactions could occur).

As it was mentioned above, the reactions between $^{\bullet}CH_2$–COOH radical and oxygen are much faster than the reaction between the C_6H_5–$^{\bullet}S$ radical and oxygen. However, because of the lack of significant concentrations of other

Scheme 4.

radicals, in the presence of oxygen, the phenylthiyl radical decays through dimerization and also through the reaction with oxygen, in spite of the rate constant for this latter reaction being quite small ($k \sim 10^4 \, M^{-1} \, s^{-1}$) [36,37].

An analogous mechanism for the direct photolysis of SBTGA is proposed (Scheme 2) and is based on the generalizations mentioned above. Three pathways of primary reactions are possible. First is C–S bond cleavage (main reaction) leading to formation of C_6H_5–$^\bullet CH_2$ ($\Phi = 0.24$ in the absence of oxygen, and $\Phi = 0.28$ in the presence of oxygen (see Table 4)) and $^\bullet S$–CH_2–$COOH$ radicals. The second pathway is another C–S bond cleavage leading to the formation of C_6H_5–CH_2-$^\bullet S$ ($\Phi \sim 0.02$ in the absence of oxygen, and $\Phi \sim 0.01$ in its presence (see Table 4)) and $^\bullet CH_2$–$COOH$ radicals. The third photolytic pathway is a C–C bond cleavage leading to the formation of C_6H_5–CH_2–S-$^\bullet CH_2$ ($\Phi \leq 0.03$ in the presence of oxygen, and $\Phi \leq 0.02$ in its absence) and $^\bullet COOH$ radicals. The limiting quantum yield of C_6H_5–CH_2–S-$^\bullet CH_2$ in deaerated solution corresponds to the quantum yield for carbon dioxide formation (0.03) (see Table 4). There is one more possibility for a bond cleavage (starting from a photoionization), but we do not observe the S-centered radical cation (C_6H_5–CH_2–$S^{\bullet+}$–CH_2–$COOH$) even in laser flash photolysis experiments. The rationalization is the same as for the lack of photoionization in the PTAA steady-state photolysis.

For the purposes of discussion, we present a shortened version of the direct photolysis mechanism of SBTGA (Scheme 4) showing only the main pathway (C–S bond cleavage). Following 254 nm irradiation of SBTGA, one of the C–S bond cleavages occurs. The same three general pathways for the fates of these radicals exist for SBTGA as enumerated above for PTTA. However, for SBTGA, the rate constants for the reactions between the C-centered radical and oxygen (compared to the S-centered radical and oxygen) are not very different. In general, aliphatic thiyl radicals react about 100 times slower ($4 \times 10^7 \, M^{-1} \, s^{-1}$ [36]) with oxygen than do C-centered radicals (2–$3 \times 10^9 \, M^{-1} \, s^{-1}$ [36]), but the aliphatic thiyl radicals/oxygen reactions are still about 1000 times faster than the reactions of aromatic thiyl radicals ($<10^4 \, M^{-1} \, s^{-1}$ [36]) with oxygen. This is the reason why, we show both peroxide radicals being formed in the same time range. We do not observe products formed from HOOC–CH_2–$SOO^\bullet$ radicals, but we do observe two products formed from C_6H_5–$CH_2OO^\bullet$ radicals, i.e., benzaldehyde and benzyl alcohol. Benzaldehyde (C_6H_5–CHO) is the main product when oxygen is present ($\Phi = 0.16$, Table 2). It is formed via both the Russell [47] and Bennett [48] mechanisms. Benzyl alcohol (C_6H_5–CH_2–OH) was formed only via a Russell mechanism.

References

[1] C. von Sonntag, H.-P. Schuchmann, The chemistry of functional groups, in: The Chemistry of Ethers, Suppl. E, Hydroxyl Groups and Their Sulphur Analogues, Part 2, Crown Ethers, Wiley, NY, 1980, pp. 923–934.

[2] I.W.J. Still, in: F. Bernardi, I.G. Csizmadia, A. Mangini (Eds.), Organic Sulfur Chemistry: Theoretical and Experimental Advances, Elsevier, Amsterdam, 1985, pp. 595–659.

[3] P.J. Kropp, G.E. Fryxell, M.W. Tubergen, M.W. Hager, G.D. Harris, T.P. McDermott, R. Tornerovelez, J. Am. Chem. Soc. 113 (1991) 7300–7310.

[4] S.A. Fleming, A.W. Jensen, J. Org. Chem. 61 (1996) 7040–7044.

[5] D. Vialaton, C. Richards, J. Photochem. Photobiol. A Chem. 136 (2000) 169–174.

[6] M.C. Manning, K. Patel, R.T. Borchardt, Pharm. Res. 6 (1989) 903–918.

[7] J.L. Cleland, M.F. Powell, S.J. Shire, Rev. Ther. Drug Carrier Syst. 10 (1993) 307–377.

[8] A.G. Griesbeck, M. Oelgemöller, Synlet (2000) 71–72.

[9] A.G. Griesbeck, M. Oelgemöller, J. Lex, A. Haeuseler, M. Schmittel, Eur. J. Org. Chem. (2001) 1831–1843.

[10] A. Wrzyszczynski, P. Filipiak, G.L. Hug, B. Marciniak, J. Paczkowski, Macromolecules 33 (2000) 1577–1582.

[11] R.S. Davidson, K. Harrison, P.R. Steiner, J. Chem. Soc. C (1971) 3480–3482.

[12] D.R.G. Brimage, R.S. Davidson, P.R. Steiner, J. Chem. Soc. Perkin I (1973) 526–529.

[13] E. Andrzejewska, G.L. Hug, M. Andrzejewski, B. Marciniak, Macromolecules 32 (1999) 2173–2179.

[14] E. Andrzejewska, G.L. Hug, M. Andrzejewski, B. Marciniak, Nukleonika 45 (2000) 83–91.

[15] P. Filipiak, G.L. Hug, I. Carmichael, A. Korzeniowska-Sobczuk, K. Bobrowski, B. Marciniak, J. Phys. Chem. A 118 (2004) 6503–6512.

[16] P. Filipiak, G.L. Hug, K. Bobrowski, B. Marciniak, J. Photochem. Photobiol. A Chem. 172 (2005) 322–330.

[17] S.L. Murov, I. Carmichael, G.L. Hug, Handbook of Photochemistry, Marcel Dekker, New York, NY, 1993, 124.

[18] M.D. Thomas, G.L. Hug, Computers Chemitsry, 22, Elsevier Science Ltd., 1998, 491.

[19] V. Nagarajan, R.W. Fessenden, J. Phys. Chem. 89 (1985) 2330.

[20] I. Carmichael, G.L. Hug, J. Phys. Chem. Ref. Data 15 (1986) 1.

[21] J.K. Hurley, H. Linschitz, A. Treinin, J. Phys. Chem. 92 (1988) 5151.

[22] UV Atlas of Organic Compounds, vol. IV, Butterworth, London, 1968, p. D8/8.

[23] C.N.R. Rao, Ultra-Violet and Visible Spectroscopy. Chemical Applications, Butterworth, London, 1975, p. 81.

[24] V. Talrose, A.N. Yermakov, A.A. Usov, A.A. Goncharova, A.N. Leskin, N.A. Messineva, N.V. Trusova, M.V. Efimkina, in: P.J. Linstrom, W.G. Mallard (Eds.), UV/Visible Spectra in NIST Chemistry WebBook, NIST Standard Reference Database Number 69, National Institute of Standards and Technology, Gaithersburg, MD, March 2003, p. 20899.

[25] A. Korzeniowska-Sobczuk, G.L. Hug, I. Carmichael, K. Bobrowski, J. Phys. Chem. A 106 (2002) 9251.

[26] M. Ioele, S. Steenken, E. Baciocchi, J. Phys. Chem. A 101 (1997) 2979.

[27] A. Ouchi, Y. Koga, M.M. Alam, O. Ito, J. Chem. Soc. Perkin Trans. 2 (1996) 1705.

[28] C. Chatgilialoglu, D. Griller, M. Guerra, J. Phys. Chem. 91 (1987) 3747.

[29] T.E. Eriksen, J. Lind, Radiochem. Radioanal. Lett. 25 (1976) 11.

[30] R.J. Hugemann, H.A. Schwarz, J. Phys. Chem. 71 (1967) 2694.

[31] J. Wendenburg, H. Möckel, A. Granzow, A. Henglein, Z. Naturforsch. B 21 (1966) 632.

[32] A. Wrzyszczynski, J. Bartoszewicz, G.L. Hug, B. Marciniak, J. Paczkowski, J. Photochem. Photobiol. A Chem. 155 (2003) 253.

[33] K.-D. Asmus, M. Bonifačić, Sulfur-centered reactive intermadiates as studied by radiation chemical and complementary techniques, in: Z.B. Alfassi (Ed.), S-Centered Radicals, John Willey & Sons Ltd., Chichester, 1999, pp. 141–191 (Chapter 5).

[34] G.G. Jayson, D.A. Stirling, A.J. Swallow, Int. J. Radiat. Biol. 19 (1971) 143.

[35] R. Hermann, G.R. Dey, S. Naumov, O. Brede, Phys. Chem. Chem. Phys. 2 (2000) 1213.

[36] O. Ito, Reaction of aromatic thiyl radicals, in: Z.B. Alfassi (Ed.), S-Centered Radicals, John Willey & Sons Ltd., Chichester, 1999, pp. 193–224 (Chapter 6).

[37] O. Ito, M. Matsuda, J. Am. Chem. Soc. 101 (1979) 1815.

[38] M.Z. Hoffman, E. Hayon, J. Am. Chem. Soc. 94 (1972) 7950.

[39] V.S. Chervonenko, Cand. Science, Chemistry Dissertation, Moscow, 1973.

[40] H.C. Christensen, K. Sehested, E.J. Hart, J. Phys. Chem. 77 (1973) 983.

[41] B. Maillard, K.U. Ingold, J.C. Scaiano, J. Am. Chem. Soc. 105 (1983) 5095.

[42] M.Ya. Melnikov, V.A. Smirnov, Handbook of Photochemistry of Organic Radicals, Begel House Inc., NY, 1996.

[43] E.M. Nanobashvili, G.G. Chirakadze, S.E. Gvilava, Radiation chemistry of sulfhydryl compounds, Tbilisi 2 (1980).

[44] Yu-Ran Luo, Handbook of Bond Dissociation Energies in Organic Compounds, CRC Press LLC, Boca Raton, 2003.

[45] F. Bernardi, I.G. Csizmadia, A. Mangini, Studies in Organic Chemistry, Organic Sulfur Chemistry, Elsevier, Amsterdam, 1985.

[46] T. Brinck, P. Carlqvist, A.H. Holm, K. Daasbjerg, J. Phys. Chem. A 106 (2002) 8827.

[47] G.A. Russell, J. Am. Chem. Soc. (1957) 3871.

[48] J.E. Bennett, J. Chem. Soc. Faraday Trans. 86 (1990) 3247.